Impact behavior and microstructural characteristics of PVA fiber reinforced fly ash-geopolymer boards prepared by extrusion technique

ZHANG YUNSHENG*, SUN WEI
Department of Materials Science and Engineering, Southeast University, Nanjing 210096, People's Republic of China
E-mail: zhangys279@163.com

LI ZONGJIN
Department of Civil Engineering, The Hong Kong Univesity of Science and Technology, Clear water Bay, Kowloon, People's Republic of China

Published online: 9 March 2006

A short PVA fiber reinforced fly ash-geopolymer boards (SFRFGBs) manufactured by extrusion technique is developed in this study. The effects of fly ash content and fiber volume fraction on the impact behavior of SFRFGBs are also investigated. In order to better understand the impact behaviors of SFRFGBs with different content of fly ash and fiber, Laser particle size analysis (LSA), X-ray diffraction analysis (XRD), Scanning Electron Microscope (SEM), Mercury intrusion porosimetry (MIP) are employed to explore the microstructure and failure mechanism. The experimental results show the addition of PVA fiber changes the impact failure mode from a brittle pattern to ductile pattern, resulting in a great increase in impact toughness for SFRFGBs with high volume fraction of fiber. SFRFGBs without or with low percentage of fly ash possess very high impact strength and stiffness. However, when too much fly ash was incorporated, the impact resistance of SFRFGBs is reduced obviously. This can be explained by the fact that low percentage of fly ash addition significantly improved the extrudability of fresh Geopolymer composites, resulting in a formation of very dense and compacted matrix with high-quality finish. When too much fly ash is added, the Geopolymer product is greatly reduced, resulting in a formation of very poor matrix.

1. Introduction

Recent years have seen a great development in a new generation of high performance inorganic binder—Geopolymers around the world. Geopolymers are three dimensional alumino-silicate binder materials, which were firstly discovered by J. Davidovits in the later 1970s and called it Geopolymers [1]. Geopolymer materials can be synthesized by mixing alumino-silicate reactive materials (such as metakaolin) and concentrated alkaline solutions (such as NaOH or KOH), then curing at room temperature. Under a strong alkaline solution, alumino-silicate reactive materials are rapidly dissolved into solution to form free SiO_4 and AlO_4 tetrahedral units. With the development of reaction, water is gradually split out and these SiO_4 and AlO_4 tetrahedral clusters are linked alternatively to yield polymeric precursors ($-SiO_4-AlO_4-$, or $-SiO_4-AlO_4-SiO_4-$, or $-SiO_4-AlO_4-SiO_4-SiO_4-$) by sharing all oxygen atoms between two tetrahedral units, and thereby forming monolithic like geopolymers [2].

Geopolymers made with reasonable mix-design and formulation can exhibit superior properties to Portland concrete [3–6]:

The production of geopolymers doesn't require high temperature as Portland cement. Geopolymers can be formed at ambient temperature. In addition, CO_2emission from the production process is 80%–90% less than Portland cement. Reasonable strength can be gained in a short period at room temperature. In most cases, 70% of the final compressive strength is developed in the first 4 h. Low permeability, comparable to natural granite, is another property of geopolymers. It is also reported that

*Author to whom all correspondence should be addressed.
0022-2461
DOI: 10.1007/s10853-006-6293-5

TABLE I Chemical compositions of raw materials

Raw materials	SiO_2	Al_2O_3	Fe_2O_3	CaO	MgO	TiO_2	MnO	K_2O	P_2O_5	SO_3	L.O.I
Metakaolin	62.97	26.91	2.62	0.60	–	1.24	0.01	0.18	0.74	–	4.44
Fly ash	60.70	24.72	6.90	0.70	1.13	–	–	–	–	1.50	2.35

resistance to fire and acid attacks for geopolymers are substantially superior to those for Portland cement.Apart from their high early strength, low permeability and good fire and acid resistance, geopolymers also attain higher unconfined compressive strength and shrink much less than Portland cement. Other documented properties include good resistance to freeze-thaw cycles as well as excellent solidification of heavy metal ions contained within the geopolymeric structure.

These properties make geopolymers a strong candidate for substituting Portland cement applied in the fields of civil, bridge, pavement, hydraulic, underground and military engineering [7].

Extrusion is an important plastic forming process that consists of pushing a viscous, dough-like plastic mixture through a shaped die under high compressive and high shear forces generated by extruder. The process is continuous and simpler to use than other commonly used methods (Casting, Slurry infiltration, Spray suction, Hatschek process), making it most suitable for industrial mass production. In addition, Extrusion technique enables intractable substances to be shaped into various products of complicated cross-section with minimal water content which is critical in developing high strength, low permeability and excellent durability of products [8–25].

Fly ash is a by-product with pozzolanic reactivity from coal-fired Power stations. Millions of tons of it are generated each year around the worlds. Only in china, the total amount of fly ash was accumulated up to 4 billion tons in 2002, which occupied about 4000 to 5000 hectares of areas, and 200 million or more tons are still created each year. However, less than 30% of fly ash is effectively used. In order to increase the percentage applied, the use of fly ash as partial replacement of metakaolinite to synthesis Geopolymer is systematically investigated in this study.

Fiber reinforcement has been employed in various hardened binder to improve flexural, impact behavior, toughness, and to shift failure mode. The use of short fiber is very preferable due to the simplicity and economical nature in fabrication. Considering the quasi-brittle characteristics of hardened geopolymers, PVA short fiber is incorporated to improve the low ductility of geopolymers in this study.

In this paper, a PVA short fiber reinforced fly ash-geopolymer boards (SFRFGBs) manufactured by extrusion technique is developed. The effects of fly ash and fiber on the flexural behavior of SFRFGBs are also investigated. In order to elucidate the difference in flexural behaviors of SFRFGBs, SEM-EDXA technique is employed to explore the failure mechanism in microscopic scale.

2. Materials

Metakaolin used in this study was obtained by calcining pure kaolin at 700° for 12 h. Grade I fly ash, similar to Class F fly ash according to ASTM, was supplied by Qingzhou power plant, Hong Kong, P.R.China. Chemical grade NaOH and sodium silicate solution with the molar ratio of SiO_2 to Na_2O of 3.2 were used as reagents. Two types of silica sand (600–300 μm and 150–90 μm in diameter) with the ratio of 0.6:0.4 and totally 32.5% by weight of the binder system were used as aggregate. Short polyvinyl alcohol (PVA) fiber was used as reinforcement materials. The fiber length is 6 mm with an average diameter of 14 μm and a density of 1300 kg/m^3. The average tensile strength and elastic modulus of the fiber were 1500 MPa and 36 GPa. Distilled water was used throughout.

The chemical compositions and physical properties of raw materials were listed in Table I.

3. Mixture proportions and specimen preparation

3.1. Mixture proportions

The formula of SFRFGBs used to investigate the effect of fly ash and fiber on physical and mechanical behavior is summarized in Table II. Fb1 and Fb2 are used to determine the effect of fiber volume fraction. FA10 to FA50 are to explore the effect of fly ash content. The mixture proportion of the pure SFRFGBs without fly ash and fiber (Fb0) served as a control sample is listed as follows:

$$\frac{\text{molar}SiO_2}{\text{molar}Al_2O_3} = 4.5, \quad \frac{\text{molar}Na_2O}{\text{molar}Al_2O_3} = 0.8,$$
$$\frac{\text{molar}H_2O}{\text{molar}Na_2O} = 6.4$$

The control mixture is an optimized geopolymeirc one. The details can be seen in our article [26].

3.2. specimen preparation

To uniformly disperse PVA fibers, fibers and metakaoline powder were first dry-mixed for 3 min in a planetary mixer with high shear model. NaOH, sodium silicate solution and water were mixed in a glass beaker and cooled up to room temperature. The cooled alkaline solution was

TABLE II Mixture proportions of SFRFGBs

Batches	Powder constituents of geopolymer binders: Metakaolin (%)	Fly ash (%)	Sand volume fraction (%)	Fiber volume fraction (%)
Fb0	100	0	32.5	0
Fb1	100	0	32.5	1
Fb2(or FA0)	100	0	32.5	2
FA10	90	10	32.5	2
FA30	70	30	32.5	2
FA50	50	50	32.5	2

then added into pre-mixed metakaolin powder plus fibers, and mixed for another 3 min. herein it is important to point out that the premix of NaOH and sodium silicate solution, rather than the direct addition of NaOH powder into geopolymer pastes is a key to ensure a enough long pot life to conduct the extrusion process.

The mixed, dough-like, fresh geopolymer composites were then fed into the pugmill chamber of a single-screw vacuum extruder (PVL100.3, KEMA). The barrel of the extruder was 100 mm in diameter. After further mixing, de-airing, and compaction in the extruder, the composites were pushed through a thin sheet die with a cross-sectional size of 75×6 mm. The extrudates were then covered with a plastic sheet. After 24 h, the extrudates were placed in an isothermal testing chamber and were cured at standard curing condition of 20°C and 99% RH for 28 days before testing. The hardened geopolymer sheet is cut with a diamond saw into 200×75×6 mm plates for flexural test.

4. Test methods

4.1. Impact test

Plate specimens with the dimensions of 75 × 90 × 6 mm were prepared for impact tests on an instrument impact tester (ITR-200, RADMANA). When a test started, the punch is raised to a specific height and then push down by high-pressure gas. The average velocity of the punch before and after impact is adjusted to approximately 3 m/s. The peak resistant load, fracture energy, and load gradient of the specimen can be measured and recorded. These parameters provide useful indices for impact strength, toughness, and stiffness of the specimen.

4.2. Laser particle size analysis (LSA)

To measure the particle size of raw materials, about 2 g of powder materials (metakaoline, silica fume, fly ash or slag) were added to a 100 ml beaker fully filled with water. About 0.5 g of sodium diphosphate ($Na_4P_2O_7$), serving as dispersant, was added into the beaker to increase the dispersability of the materials. After a few minutes of vibration, the dispersed sample was poured into the chamber of the LS particle Analyzer (Coulter LS2300) for testing. The testing duration was limited to 10 min to avoid the possible hydration of the sample particles. The data were recorded and analyzed automatically with Zirconia model by computer.

4.3. Microstructure analysis

X-ray diffraction analysis (XRD), Scanning Electron Microscope (SEM) and Mercury intrusion porosimetry (MIP) were employed to examine the microstructure characteristics of the SFRFGBs.

4.3.1. XRD

For the XRD test, samples from different batches were finely crushed and collected at 28 days, and then these crushed fractions were immersed for about 3 days in an acetone to stop the further hydration process and removed free water, subsequently oven-dried at 50°C for 12 h. to eliminate the absorbed water. After that, these geopolymer fractions were further ground into very fine particles, and sieved to remove most of the quartz sand. Therefore the diffraction lines representing quartz tuned out to vary quite a bit from sample to sample. This is an artifact that does not influence interpretation of the results of the present study and therefore it will be ignored.

X-ray powder diffraction was recorded on a Philips PW1830 spectrometer using CuKα Radiation with a scanning rate of 1° per min from 10° to 80°(2 θ). The wavelength was selected as 15.40562 nm (Cu).

4.3.2. SEM

A JEOL-6300 SEM microscope is used to examine the microstructure of the fractured composites at the accelerating voltage of 15 kV. These samples that are used to conduct SEM observation are firstly dried at 60°C until the constant weight is reached. Then, these samples are bonded on the sample holders with conducting glue, followed by 30 min sputter coating of carbon. After that the morphologies of the final products in samples are observed at microscopic level using SEM.

4.3.3. MIP

An Autopore IV 9500 MIP was used for to investigate the porosity and pore size distribution of different geopolymers. The samples with the size of approximate 10 mm × 10 mm × 10 mm were obtained by cutting up the harden geopolymer pastes at the age of 28 days. These samples were first oven-dried for 24 h at 50°C to remove the physically absorptive water in capillary, and then were placed into the glass penetrometer with the volume of 5 cc. After that, low pressure test was performed, followed by high pressure test (the maximum mercury press reaches 30000 psi). The intrusion and evacuation of mercury was automatically controlled by computer with Autopore IV 9500 program. The cumulative intrusion and differential

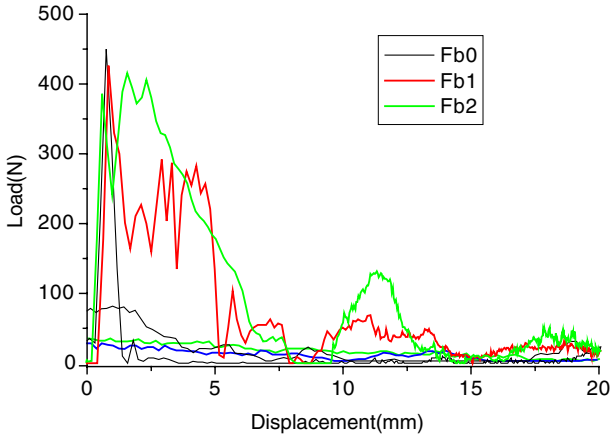

Figure 1 Impact curves of geopolymer extruded plates with different volume fraction of fiber in normally curing condition.

pore volume vs pore diameter were also measured and recorded with an increase of the pressure. The diameters of the pores intruded by the mercury were calculated using "Washburn equation", with a mercury contact angle of 130 degree.

5. Results and discussions

Figs. 1 and 2 show the impact response curves of SFRFGBs with different percentages of fly ash and fiber. To compare the effect of fiber and fly ash content on the impact behaviors, Fb0 without fiber and fly ash is served as control sample. Fb1 to Fb2 are used to investigate the effect of the volume fraction of PVA fiber. FA10 to FA50 are designed to study the effect of fly ash content. The mixture proportions of various SFRFGBs are listed in Table I. The impact strength, stiffness and toughness for Fb0 to FA50 are also shown in Table III.

As can be seen in Fig. 1, Fb0 has highest impact strength (449.7N), while the impact displacement is very small, only around 0.84 mm. And after peak load, Fb0 specimen can not sustain any loading, resulting in a sharp drop

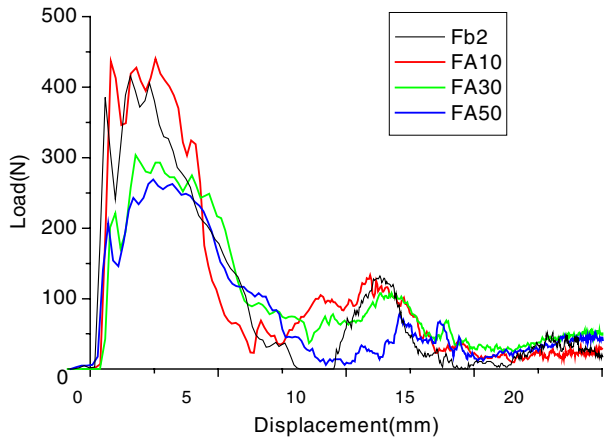

Figure 2 Impact curves of geopolymer extruded plates with different percentages of fly ash in normally curing condition.

TABLE III Impact resistance of geopolymer extruded plates for normally curing condition

Batches	Impact strength (N)	Impact stiffness (N/mm)	Impact toughness (mJ)
Fb0	449.7	1150	209
Fb1	426.0	873	1177
Fb2(or FA0)	429.6	749	1833
FA10	443.3	1007	2108
FA30	290.0	665	1587
FA50	268.8	456	1307

of its impact curve. This indicates that geopolymer plate without fiber will be broken without any warning when the peak load is reached. This may be very dangerous for practical construction. Fb0 specimen is separated into 5 small fractions during impact test. The fracture pattern is typically of a brittle failure.

When 1% PVA fiber is incorporated (Fb1), the impact response curve takes on a new look. Unlike Fb0, the impact curve of Fb1 doesn't directly fall down to 0 after peak load, rather than only drops to about 300 N and sustains the load for a long displacement. This indicates the addition of PVA fiber prevent the cracks from rapid propagating, thus an increase in ductility. However, 1% fiber is so little that they can only bear a part of the whole impact load. The geopolymer plate with 1% fiber is broken into 3 small pieces after subjecting to impact test. This suggests that the geopolymer plate with 1% fiber shows some characteristics of ductile materials.

When 2% PVA fiber is incorporated (Fb2), the impact curve shows an obvious strain hardening response after peak load. Fb2 sample can sustain the peak load (429.6N) up to around 2.5 mm of displacement. After that the bearing capacity falls slowly up to 7.5 mm of displacement. No crack is found on the surface of geopolymer plate with 2% of PVA fiber. Only a hole caused by the high speed impact of punch was seen in the center of sample after the impact test. This demonstrates that 2% fiber can ensure the integrality of geopolymer plate near the hole in the case of a large deflection caused by high speed impact of the punch.

By comparing the impact test results in Table II, it can be seen that the addition of fiber show a decreasing trend for the impact strength (peak load), however the reduction is very little, only 5.3% for Fb1 and 4.47% for Fb2. In contrast, a great influence of fiber content is clearly seen on impact stiffness (gradient in linear section for impact curves) and impact toughness (area between impact curves and the x-axis), especially for the latter. For example, the impact toughness of Fb1 and Fb2 is 4.63 and 7.77 times higher than that of Fb0.

Fly ash was vastly produced as by-product from the thermal power plants across the world. Due to good pozzolanic reactivity, fly ash is widely used to partially replacement of Portland cement in the filed of civil engineering. Considering that fly ash contains an

amount of reactive Al_2O_3 and SiO_2, which are similar to metakaoline, a part of metakaoline is replaced by fly ash. Fig. 2 shows the impact response curves for extruded geopolymer plates with different percentages of fly ash at the same fiber content (FA10, FA30 and FA50). The impact test results are also shown in Table II. As can be seen in Fig. 2 and Table II, the impact resistance is a function of the percentages of fly ash. When 10% by weight of fly ash is added (FA10), not only are the impact strength and stiffness enhanced, but also is the toughness (absorbed energy) increased from 1833 mJ to 2108 mJ. When too much fly ash are incorporated into geopolymer mixture (FA30 and FA50), the impact resistance of geopolymer extruded plates is reduced rapidly, and the reducing percentage is increased with an increase in the percentages of fly ash. It is especially true for 50% of fly ash addition. For instance, when comparing with Fb2 the impact strength, stiffness and toughness of FA50 are reduced by 37.4%, 39.1% and 28.7%, respectively.

As mentioned above, 10% fly ash addition enhances the impact resistance of geopolymer extruded plate. The enhancing mechanism of fly ash is investigated by the particle size distribution (PSD), Scanning Electron Microscope (SEM) examination, X-ray diffraction (XRD) analysis, and MIP (Mercury intrusion porosimetry). Fig. 3 shows the Particle size distributions of various types of raw materials. It can be seen in Fig. 3 that coarse sand has the largest particle size amongst the four raw materials, then fine sand. Metakaoline and fly ash have the smallest particle size, which fill in voids among sands, resulting in a compacted system. Although the particle size of fly ash is very closed to that of metakaoline particle, the spherical shape of fly ash greatly improve the extrudability of geopolymer mixture, as a result a very highly quality extrudates are produced. In addition, the particles of fly ash are also served as the nucleation sites of geopolymerization reaction, which promotes the reaction rate and the formation of geopolymer products. The phenomenon can also be confirmed by comparing the amorphous areas of XRD spectral for pure geopolymer without fly ash (Fb2)

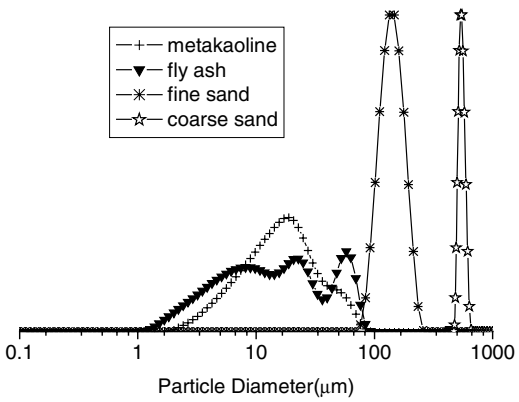

Figure 3 Particle size distributions of metakaoline, fly ash, fine and coarse sand.

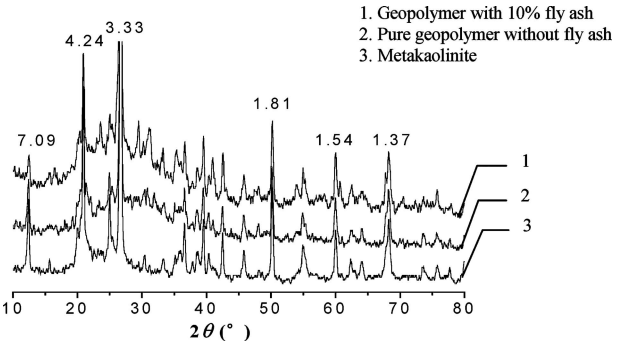

Figure 4 X-ray diffractograms of Metakaolin, pure geopolymer, and fly ash based geopolymer.

and Geopolymer with 10% fly ash (FA10), as shown in Fig. 4.

As can be seen from Fig. 4, both pure geopolyme and fly ash based geopolymer have a large diffuse halo peak at about 20–40°($2\theta_{max}CuK_{\alpha}$). This means that geopolymers with or without fly ash are mainly X-ray amorphous materials consisting of randomly developed Si-Al polyhedra with a lack of periodically repeating Si-Al atomic ordering. Comparing the area under X-ray diffractogram at 20–40°, it is found that fly ash based geopolymer shows larger area than pure geopolymer without any fly ash, which indicates fly ash based goepolymer contains more amorphous products than pure geopolymer. In addition, several sharp characteristic peaks (7.09 Å, 4.23 Å, 3.33 Å, 1.81 Å, 1.54 Å, 1.37 Å) are also seen from Fig. 4. According to the XRD-pattern, these peaks are identified as quartz and kaolin. With respect to X-ray diffractogram of metakaolin, kaolin and quartzes are induced by metakaolin, and in the process of geopolymerization, the kaolin and quartzes don't take part in reaction.

Figs 5 and 6 show the SEM images for FA0 and FA10, respectively. Some small pores and cracks can be easily found in FA0, while the microstructure of FA10 with 10% fly ash is much denser. If too much fly ash is added into geopolymer, the microstructure of hardened Geopolymer (FA50) will become relatively loose Fig. 7. This can be attributed to the fact that no enough geopolymer products are formed in the interspaces amongst sands due to too less high reactive metakaoline.

The influence of fly ash content on porosity and pore size distribution of hardened geopolymer can also obviously be seen in Figs. 8 and 9. It can be seen from Fig. 8 that the addition of 10% fly ash greatly reduced the total porosity. This is deemed to be responsible for the denser and compacted microstructure of geopolymer, which is consistent with the observation of SEM images. In contrast, when 50% fly ash is incorporated into geopolymer mixture, the hardened matrix shows a very high the porosity, thus a formation of some large pore and cracks, which is also be confirmed by observing Fig. 7.

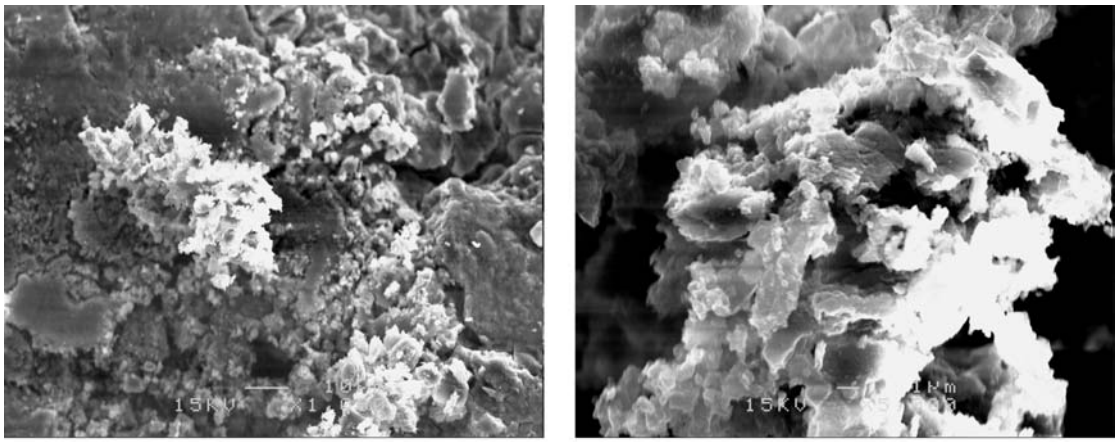

(a) Low magnification micrograph (b) high magnification micrograph

Figure 5 SEM images of geopolymer with no fly ash addition (FA0).

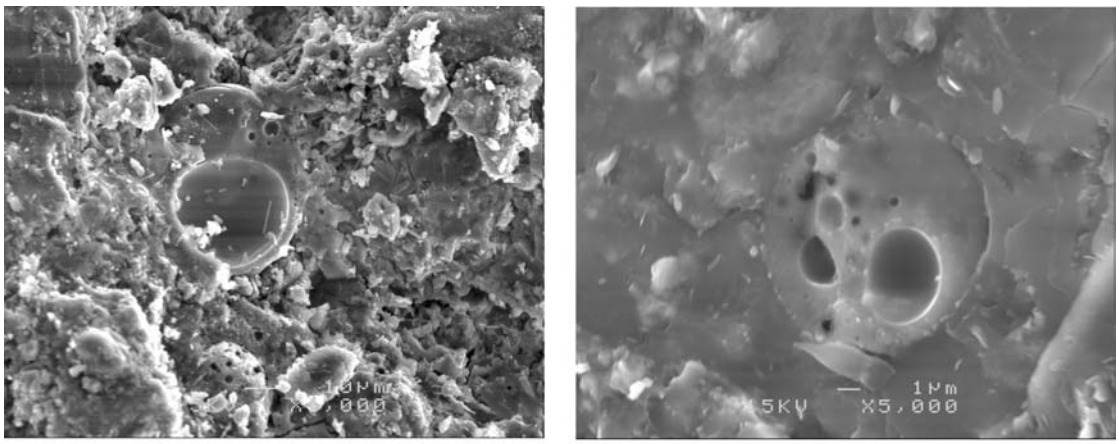

(a) Low magnification micrograph (b) high magnification micrograph

Figure 6 SEM images of geopolymer with 10% fly ash addition (FA30).

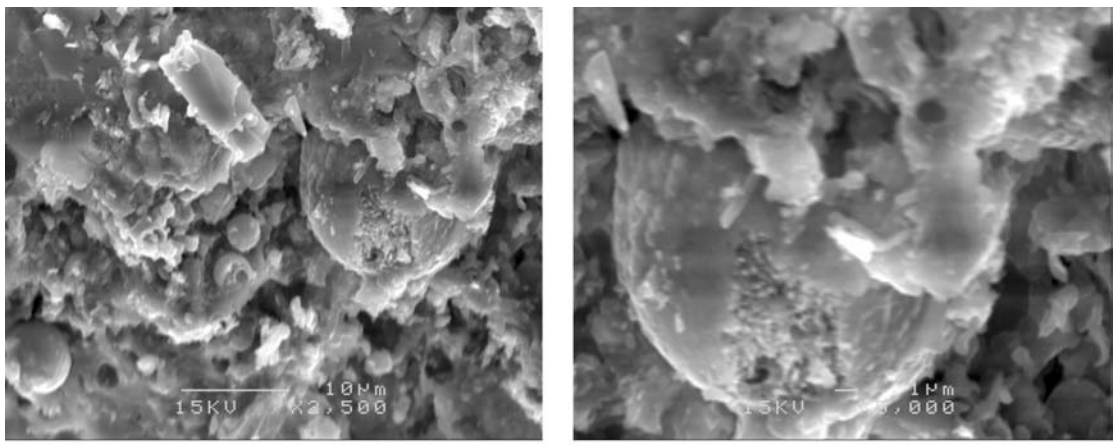

(a) Low magnification micrograph (b) high magnification micrograph

Figure 7 SEM images of geopolymer with 50% fly ash addition (FA50).

Fig. 9 gives the cumulative intrusion and its distribution of various geopolymers with different percentage of fly ash. By comparing with the mercury intrusion curves, cumulative pore volume with pore diameter smaller than 495 nm accounts for 60% of the total porosity for Fb2 sample without fly ash replacement, 90% for FA10, and 55% for FA50. This indicates that the addition of 10% of fly ash obviously reduces the pore size and improves pore structure in hardened geopolymer. However, too much fly ash addition will increase the percentage of

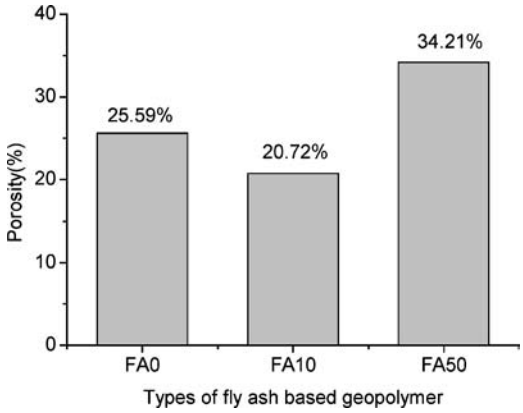

Figure 8 Porosity of different geopolymers.

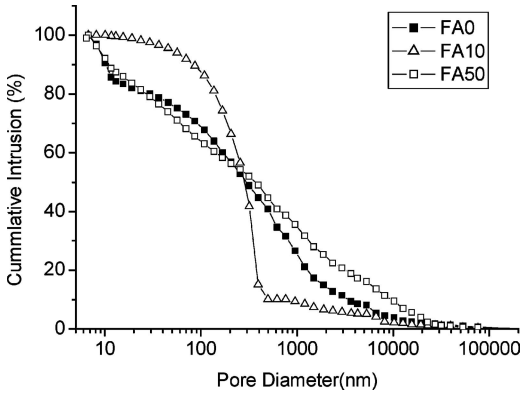

Figure 9 Mecury intrusion curves of different geopolymers.

large size pore, leading to the formation of poor structure. The results are good agreement with above SEM observations.

6. Conclusion

1. The addition of high volume fraction PVA fiber changes the impact failure mode of fly ash-geopolymer boards from a brittle pattern to ductile pattern, resulting in a great increase in impact toughness.

2. Short PVA fiber reinforced fly ash-geopolymer boards without or with low percentage of fly ash possess very high impact strength and stiffness. However, when too much fly ash was incorporated, the impact resistance is reduced obviously.

3. The spherical shape of fly ash can greatly improve the extrudability of geopolymer mixture, resulting in the denser microstructure of the finial geopolymeric boards with low percentage of fly ash. However, when too much fly ash was incorporated, the improvement of the microstructure caused by fly ash cannot compensate the decrease of geopolymer products due to the low pozzolanic reactivity of fly ash in case of high percentage of fly ash. As a result, the microstructure of fly ash-Geopolymer boards becomes relatively loose.

Acknowledgments

Authors gratefully acknowledge the financial support from the china national natural science foundation (No. 50278018), Opening and flowing research project funded by Nanjing Hydraulic Research Institute (No.Yk90508), Laboratory for Silicate Materials Engineering of Wu Han University of Technology (No. SYSJJ2004-02) and Jiang Su Province Natural Science Foundation (BK2005216). Some of the research was carried out at material laboratory, Department of Civil Engineering, Hong Kong University of Science and Technology.

References

1. J. DAVIDOVITS, *J. Therm. Anal.* **35**(2) (1989) 429.
2. J. DAVIDOVITS and M. DAVIDOVITS, "Geopolymer: Ultrahihg-Temperature Tooling Material for the Manufacture of Advanced Composites," edited by R. ADSIT and F. Gordaninejad, 36th Annual SAMPE Symposium and Exhibition, Covina (CA, USA, 1991) Vol. 36 pt 2, p. 1939.
3. J. DAVIDOVITS, "Geopolymer Cement to Minimize Carbon-Dioxde Greenhouse-Warming", edited by M. Moukwa, SL. Sarkar, K. Luke and MW Grutzeck, *Ceram. Trans.* **37**(1993) 165.
4. J. DAVIDOVITS, Properties of Geopolymer Cemen, In Škvára F. Proceedings 1st International Conference on Alkaline Cements and Concretes, Kiev Ukraine: Scientific Research Institute on Binders and Materials, Kiev State Technical University (1994) p. 131.
5. R. E. LYON, A. FODEN, P. N. BALAGURU, M. DAVIDOVITS and J. DAVIDOVITS, *J. Fire Mater.* **21**(2) (1997) 67.
6. J. DAVIDOVITS. in "American Concrete Insititue," edited by P. K. Mehta Detroit, (1994) Vol. SP-144, p. 383.
7. J. DAVIDOVITS, Geopolymer chemistry and properties, in J. Davidovits and J. Orlinsl, Proceedings of the First European Conference on Soft Mineralogy, Compiegne (France: The Geopolymer Institute, 1988) Vol. 1, p. 25.
8. Y. SHAO, S. MARIKUNTE and S. P. SHAH, *Concr. Intern.* **17**(4) (1995) 48.
9. Y. SHAO, S. MARIKUNTE and S. P. SHAH, "High Performance Fiber-Cement Composite by Extrusion Processing. Materials for the New Millenium," edited by K. P. Chong, Proceedings of the 4th Materials Engineering Conference, Washington, D.C., (1996) Vol. 2, p.25.
10. LI ZONGJIN, MU BIN and N. C. CHUI. STANLEY, *ACI Mater J* **96**(5) (1996) 574.
11. LI ZONGJIN, MU BIN and N. C. CHUI STANLEY, *J. Mater Civil Eng.* **13**(4) (2001) 248.
12. YIXIN SHAO and S. P. SHAH, *ACI Mater. J.* **94**(6) 555.
13. A. CORINA, S. MARIKUNTE and S. P. SHAH, *Adv. Cement Based Mater.* **8** (1998) p. 47.
14. LI ZONGJIN and MU BIN, *J. Mater. Civil Eng. ASCE* **10** (1998) 2.
15. H. STANG and C. PEDERSON, in Proceedings of the 4th Materials Engineering Conference, Washington, D.C. (1996) Vol. 2, p. 261.
16. M. J. STEVENS, in "Extruder Principles and Operation" (Elsevier Applied Science, London, 1985).
17. H. STANG and V. C. LI, Extrusion of ECC-Material, in Proceedings of the 3th International Workshop on HPFRCC3, edited by H.W. Reinhardt and A. E. Naaman, (1999), p. 203.
18. SHAO YINXIN, QIN JUN and S. P. SHAH, *Cement Concr. Res.* **31** (2001) 1153.
19. LI ZONGJIN and MU BIN, *J. Amer. Ceram. Soc.* **84**(10) (2001) 2343.
20. S. P. SHAH, A. PELED, D. DEFORD, *et al.*, "Extrusion Technology for the Production of Fiber-Cement Composites", edited by A. A. Moslemi, in Proceeding of Inorganic-Bonded Wood and Fiber composite Materials, Forest Products Society: Idaho. USA (1998) Vol. 6, p. 261.

21. ALVA PELED and SURENDRA P SHAH, *J. Mater.Civil Engng.* **15**(2) (2003) 192.
22. Y. AKKAYA, A. PELED and S. P. SHAH, *Mater. Struct.* **33** (2000) 515.
23. S. IGARASHI, A. BENTUR and S. MINDESS, *Cement Concr. Comp.* **18** (1996) 313.
24. A. PELED, Y. A. AKKAYA and S. P. SHAH, in "Effect of Fiber Length in Extruded and Cast Cement Composites," ACI SP-190 on High Performance Concrete Fiber Reinforced Thin Products, edited by A. Peled, S.P. Shah and N. Banthia (American Concrete Institute, Detroit, 2000) p. 1.
25. A. PELED, M. F. CYR and S. P. SHAH, *ACI Mater. J.* **97**(5) (2000) 509.
26. YUNSHENG ZHANG, WEI SUN and ZONGJIN LI, Preparation and Characterization of Na-PSS Geopolymer, The First China National Workshop on Chemically Activated Cementing Materials, Nanjing (2004) p. 244.

Received 1 June
and accepted 19 August 2005